Mitigation of self-excited oscillations at full load: CFD analysis of air admission and effects of runner design

D. Chirkov[1], P. Scherbakov[2], S. Cherny[1], A. Zakharov[3], V. Skorospelov[4], P. Turuk[4]

[1]Institute of Computational Technologies SB RAS, Novosibirsk, Russia
[2]Novosibirsk State University, Novosibirsk, Russia
[3]OJSC "Power Machines" LMZ, St-Petersburg, Russia
[4]Sobolev Institute of Mathematics SB RAS, Novosibirsk, Russia

chirkov@ict.nsc.ru

Abstract. In full and over load operating points some Francis turbines experience strong self-excited pressure and power oscillations, which restrict the range of operation and maximum output of the turbine. Previously the authors proposed a 1D-3D two-phase model and numerical method for investigation of this phenomenon. In the present paper this model is further extended and applied to investigation of countermeasures, used for prevention of high load oscillations. First, the third phase – non-condensable air – is introduced into the model in order to investigate the effect of air admission. Then, several modifications of runner cone are examined, showing negligible effect on the amplitude and frequency of full load oscillations. Next, different modifications of runner blade shape are considered, giving different axial and circumferential velocity profiles downstream the runner. It is shown that variation of blade shape significantly affects the onset and intensity of self-excited oscillations. The obtained results indicate that proper runner design is able to eliminate high load instability without the need of air admission and reduction in turbine efficiency.

1. Introduction

The paper is devoted to CFD investigation of remedies, used to mitigate self-excited oscillations in Francis turbines in high load operating points. It is well known, that operation of Francis turbines in full load and overload regimes can exhibit synchronous pressure pulsations that propagate along the whole water conduit of the power plant [1,2,3]. This effect significantly restricts operation of Francis turbines at high discharge, limiting the maximum power output. The reason of these pulsations is a hydrodynamic instability of swirling cavitating flow in the draft tube cone in full load operating conditions.

In [4, 5] we developed and validated a hybrid 1D-3D model and numerical approach for simulation of this phenomenon. The model consisted of 1D hydro-acoustic equations for the penstock and 3D Reynlolds-Averaged Navier-Stokes equations for the two-phase “liquid-vapor” flow in turbine and draft tube. Both systems of equations are linked together by pressure and discharge at the penstock-turbine interface and solved simultaneously. In [6] it was shown that this model is able to predict the onset of instability at high discharges appearing as the onset of high pressure and power oscillations.

The present paper analyses the countermeasures used to prevent or reduce self-excited oscillations. To begin with we considered aeration of flow behind the runner. In [7] it was shown that air injection through the center of runner cone can significantly reduce oscillations in part load. In [8, 9] it was shown that air injection/admission can also reduce power oscillations and unit vibrations in high load operating points. Air affects pulsations in two ways. First, the airflow changes pressure and velocity field, increasing the pressure and reducing cavitation in the center of draft tube cone. Second, it alters the compliance $C = -\partial V_c / \partial H$ of the gaseous cavity of volume V_c including water vapor and air.

In order to simulate the effect of air injection we extended the previous 2-phase model [4, 5] to 3-phase "liquid-vapor-air" model. For the beginning air is treated as incompressible [10]. The influence of air injection through the runner cone is numerically investigated. The results are promising, confirming reduction of pressure pulsations at sufficient air discharges.

CFD computations, performed in [5] showed that different runners have different amplitudes of high load pulsations, dropping a hint that proper runner design can completely remove the zone of instability and associated pressure pulsations in high load. This thought was confirmed in practice for Guri II hydro-power plant, see [11]. There the newly designed runner avoided high load pressure pulsations that were reported for the old runner. Being inspired by these results, we applied our 1D-3D model for the investigation of the effects of runner design on high load pulsations.

First, three modifications of runner cone shape are examined, since they can easily be performed on site for the existing runners. Computations showed that the shape of runner cone has almost negligible effect on the amplitude and frequency of full load oscillations. This fact indicates that the reason of instability in the draft tube is formed upstream, by the velocity profile exiting runner blades.

In order to check this idea, different runner modifications, involving blade shape and hub variations, are considered, giving different axial and circumferential velocity profiles downstream the runner. The principal requirement should be met in this analysis. Namely, all runner modifications should be comparable to the initial runner in terms of efficiency and cavitation. In order to construct the set of admissible runner shapes, fulfilling this principal requirement, we used our runner optimization tool [12]. Several runner modifications are taken from the admissible set, outperforming the initial runner in terms of efficiency and cavitation. Then, unsteady CFD computations of high load pulsations were carried out for these runners. It was found, that amplitude of pulsations for 2 of 4 runner modifications was significantly reduced. Correlation with axial and circumferential velocity profiles was also found, that can be accounted at the stage of runner design.

2. Hybrid 1D-3D three-phase model

In order to capture synchronous self-excited oscillations, propagating along the whole water system of power plant, we simulate the unsteady flow-fiend in penstock and turbine, see Fig. 1.

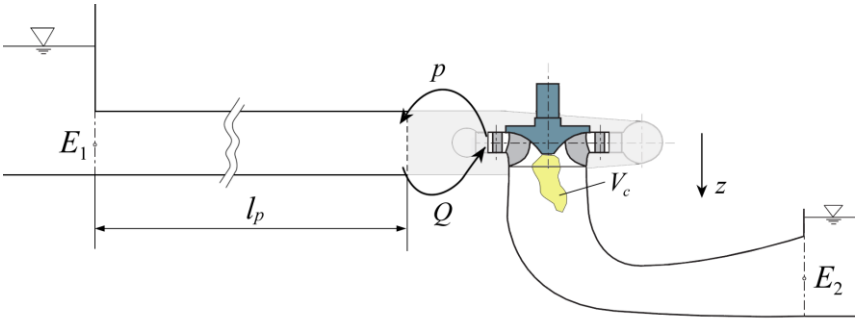

Figure 1. Computational domain for 1D-3D model.

Fluid flow in penstock is simulated using 1D hydro-acoustic equations

$$\begin{cases} \dfrac{\partial h}{\partial t} + \dfrac{a^2}{gA}\dfrac{\partial Q}{\partial x} = 0, \\ \dfrac{\partial Q}{\partial t} + gA\,\dfrac{\partial h}{\partial x} = 0, \end{cases} \qquad x \in [0, l_p]. \tag{1}$$

Here $h = p/(\rho_L g) - z$ is the piezometric head (note, that *Oz* axis is directed downwards); *Q* is the discharge; *a* is the constant wave speed, taken *a* = 1200 m/s; *A* is the cross section of penstock. Penstock domain is needed to provide correct inlet boundary conditions for turbine domain.

Cavitating flow inside the turbine with draft tube is described as isothermal homogeneous three-phase mixture, consisting of liquid, vapour, and, generally, non-condensable gas (air). Distribution of liquid volume fraction α_L is governed by transport equations with source terms, responsible for evaporation and condensation. Distribution of gas volume fraction α_G is governed by the same equation with zero source term [10]:

$$\frac{\partial \rho}{\partial t} + \operatorname{div}(\rho \mathbf{v}) = 0, \tag{2}$$

$$\frac{\partial \rho \mathbf{v}}{\partial t} + \operatorname{div}(\rho \mathbf{v} \otimes \mathbf{v}) + \nabla \hat{p} = \operatorname{div}(\boldsymbol{\tau}) + \rho \mathbf{f}, \tag{3}$$

$$\frac{\partial \alpha_L}{\partial t} + \operatorname{div}(\alpha_L \mathbf{v}) = \frac{1}{\rho_L}(m^+ + m^-), \tag{4}$$

$$\frac{\partial \alpha_G}{\partial t} + \operatorname{div}(\alpha_G \mathbf{v}) = 0. \tag{5}$$

Here $\rho = \alpha_L \rho_L + \alpha_G \rho_G + (1 - \alpha_L - \alpha_G)\rho_V$ is the mixture density; $\mathbf{v}$ is the velocity vector; $\hat{p} = p + 2\rho k/3$; *p* is the static pressure; *k* is the turbulence kinetic energy. Absolute reference frame is used for static components of turbine flow passage, while rotating reference frame is used for the runner, rotating with angular velocity ω around the *Oz* axis. Thus for runner sub-domain $\mathbf{f} = (x_1\omega^2 + 2u_2\omega,\ x_2\omega^2 - 2u_1\omega,\ g)$. Account of gravity acceleration is necessary since we consider cavitation in prototype turbine, where hydrostatic component of pressure changes significantly in the draft tube. In (3) $\boldsymbol{\tau} = \{\tau_{ij}\}$ is the tensor of viscous stresses

$$\tau_{ij} = (\mu + \mu_T)\left[\left(\frac{\partial u_i}{\partial x_j} + \frac{\partial u_j}{\partial x_i}\right) - \frac{2}{3}\delta_{ij}\frac{\partial u_k}{\partial x_k}\right].$$

Here μ is the dynamic viscosity of three phase mixture

$$\mu = \alpha_L \mu_L + \alpha_G \mu_G + (1 - \alpha_L - \alpha_G)\mu_V,$$

where μ_L, μ_G, μ_V are the dynamic viscosity coefficients of liquid, gas (air) and vapour, respectively. Turbulent viscosity μ_T is evaluated using conventional formula

$$\mu_T = C_\mu \rho \frac{k^2}{\varepsilon}, \qquad C_\mu = 0.09.$$

Note, that correction of turbulent viscosity, suggested in [13] for unsteady cavitating flows, is not used so far. Kim-Chen *k*-ε turbulence model [14] with log-law wall function on the solid walls is used to close the mean flow equations (2)-(5).

Condensation (m^+) and evaporation (m^-) terms in (4) are evaluated using the model of Zwart, Gerber, and Belamri [15]:

$$m^+ = C_{prod}(1 - \alpha_L - \alpha_G)\rho_V \sqrt{\frac{2}{3}\frac{\max[0, p - p_V]}{\rho_L}}, \qquad m^- = -C_{dest}\alpha_L \rho_V \sqrt{\frac{2}{3}\frac{\max[0, p_V - p]}{\rho_L}}, \tag{6}$$

where $C_{prod} = 3 \cdot 10^4$, $C_{dest} = 7.5 \cdot 10^4$.

It should be noted that according to (5) air is treated as incompressible fluid with constant density $\rho_G < \rho_L$. Therefore the present 3-phase model inherently cannot describe the change of cavity compliance introduced by the air. In this way our air injection is similar to water jet, considered in [16, 17], except the difference in density of injected fluid. Ideally, air injection model should account for compressibility of the air phase.

In case of there is no air injected in the system, α_G remains zero throughout the flow-field, and our 3-phase model reduces to previous 2-phase "liquid-vapor" model.

Boundary conditions, preserving total specific energy E_1 at the inlet of the penstock and total specific energy E_2 at draft tube outlet, see Fig.1, are described in [4, 5]. With these inlet/outlet conditions discharge Q is not known a priory and is found in the process of CFD computation.

For the air phase, constant air velocity w_G is specified at the runner cone in that cell faces, where $R < R_v$, see Fig. 2, 3. Pressure is extrapolated from the interior of computational domain.

3. Numerical method

The above 1D-3D three-phase model is implemented within the in-house developed CADRUN solver. Three-phase fluid flow equations (2)-(5) are solved numerically using artificial compressibility method, similar to [10]. Dual time stepping is used for unsteady calculations. In pseudotime equations are marched using implicit finite volume scheme. Third order accurate MUSCL scheme with a is used for discretization of inviscid fluxes through cell face. In order to prevent numerical oscillations, artificial dissipation is added on liquid-gas interfaces, as suggested in [10]. Second order backward scheme is applied for physical time derivatives. Linearized system of discrete equations is solved using LU-SGS iterations. All equations (2)-(5) are solved in terms of $(p,\mathbf{v},\alpha_L,\alpha_G)$ in a coupled manner. For more details reader is referred to [18]. Hybrid MPI+OpenMP parallelization of the code is used to speed up unsteady computations.

Periodic stage approach is used for turbine flow analysis, requiring computations only in one wicket gate (WG) channel, one runner channel, and the whole draft tube (DT). Mixing plane boundary condition is applied on "WG – runner" and "runner – DT" interfaces with circumferential averaging of all flow variables (p, Cr, Cu, Cz, α_L, α_G, k, ε). In [6] it was shown that this approach is quite adequate for simulation of self-excited pulsations. Hydro-acoustic equations (1) are solved using 1st order implicit finite difference scheme. In each time step equations (1) and (2)-(5) are iterated in pseudotime simultaneously until convergence. During the iterative solution of hydro-acoustic and two-phase equations flow parameters are exchanged through artificial "penstock – wicket gate" interface. Implementation of this condition is described in detail in [4].

Computational procedure is the following. First, steady state 3-phase flow-field without the penstock is computed. Then the penstock is attached and unsteady 3-phase computation is set up.

4. Influence of air injection

The effect of air injection is investigated for prototype Francis turbine with specific speed n_q=48.3. Relatively fine mesh in WG, runner and draft tube is used, consisted of 520'000 cells, see Fig. 3. Time step Δt is taken 1/48 of runner rotation period, which proved to be small enough in former two-phase computations [5]. Air density was taken ρ_G = 1 kg/m^3.

Fig. 4 shows the influence of air flow-rate on amplitude of pressure pulsations in over-load operating point P / P_{rated} = 1.175. It can be seen that low air flow-rate (Q_{air} / Q =0.001) has little effect on pressure pulsations, while with the increased air flow pressure pulsations are completely mitigated. Fig. 5, *a*, *b* illustrates multi-phase flow-field in the draft tube for the case Q_{air} / Q = 0.001 in two time moments t_1 and t_2, marked in Fig. 4. At low air flow-rate significant cavitation area is still present, and the volume of vapor cavity changes in time. Air jet with variable length is clearly seen in the centerline. Fig. 5, *c* shows the case Q_{air} / Q = 0.004. Here the flow-field is nearly the same in time, with no cavitation area and no visible air jet. Instead, air is accumulated just below the runner cone. Fig. 6 shows corresponding axial velocity distributions. It can be seen that strong air injection deviate

velocity field in the upper part of the draft tube, enlarging the stagnant recirculation zone in the central part and thus increasing static pressure. Elimination of cavitation zone removes destabilizing physical mechanisms, exciting pressure oscillations in the whole hydraulic system.

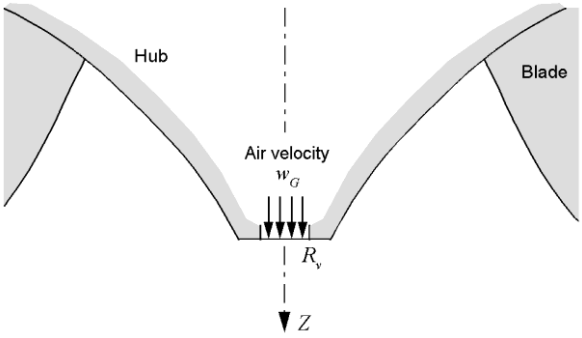

Figure 2. Aeration through runner cone.

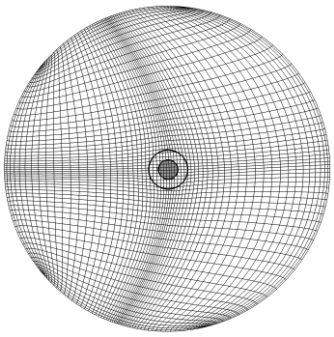

Figure 3. Mesh in draft tube inlet cross section. Grey area is the aeration hole.

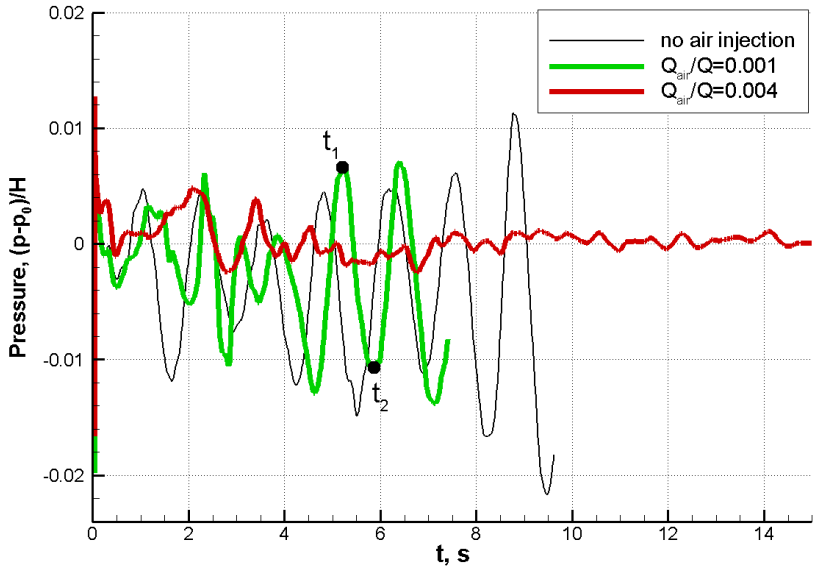

Figure 4. Pressure pulsations in WG inlet: influence of air injection.

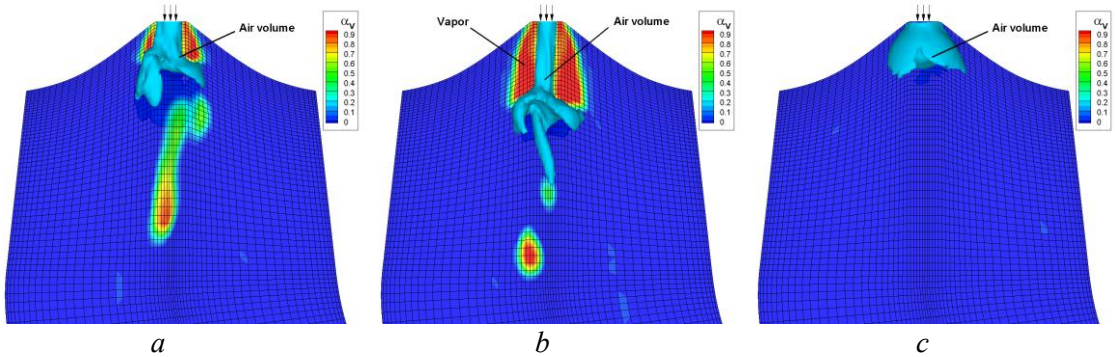

a *b* *c*

Figure 5. Distribution of vapor volume fraction $\alpha_V \equiv 1-\alpha_L-\alpha_G$ in vertical draft tube section. Air volume is visualized as iso-surface $\alpha_G = 0.25$. *a* – Q_{air}=0.001Q, $t = t_1$; *b* – Q_{air}=0.001Q, $t = t_2$; *c* – Q_{air}=0.004Q.

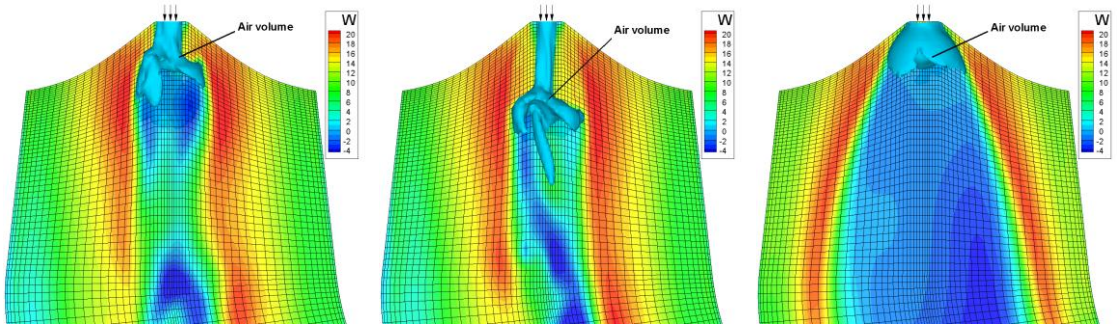

a *b* *c*

Figure 6. Distribution of axial velocity in vertical draft tube section. Air volume is visualized as iso-surface $\alpha_G = 0.25$. (*a*) – Q_{air}=0.001Q, $t = t_1$; (*b*) – Q_{air}=0.001Q, $t = t_2$; (*c*) – Q_{air}=0.004Q.

5. Variation of runner cone

Another approach to eliminate instability at high load without the need of air injection is to enhance runner design. For the beginning we examined several runner cone modifications, shown in Fig. 7. Along with the initial runner cone, three modifications were examined: v1 – short runner cone, v2 – wide cone, v3 – initial cone with cylindrical extension, see Fig. 7. These modifications of runner cone have little effect on turbine performance and can be relatively simply implemented for the existing runners on site. It should be noted, that v3 modification is proved to be useful for the reduction of vortex rope pressure pulsations in part load [8,19].

All the modifications were computed using the above 1D-3D model with no aeration ($\alpha_G \equiv 0$). Operating point is P / P_{rated} = 1.175, where the initial variant gives maximum amplitude of self-oscillations. Computations were performed with time step $\Delta t = T_n / 24$ and a coarser mesh, consisted of 153'000 cells for WG, runner and draft tube. Fig. 8 shows the resulting relative pressure pulsations, monitored in wicket gate inlet. Pressure levels are shifted for the sake of visualization. It can be seen from the figure, that all the considered runner cone modifications have negligible effect on the amplitude and frequency of pressure self-oscillations. This result indicate that conditions for instability and development of strong self-exited oscillations originate from upstream, namely from the velocity profile, exiting the runner.

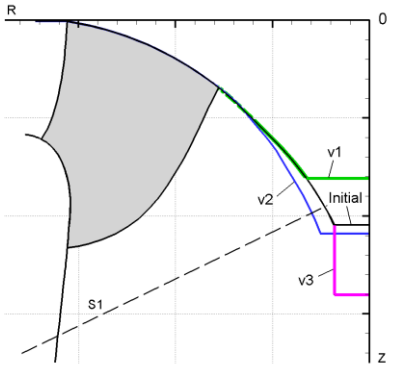

Figure 7. Runner cone modifications.

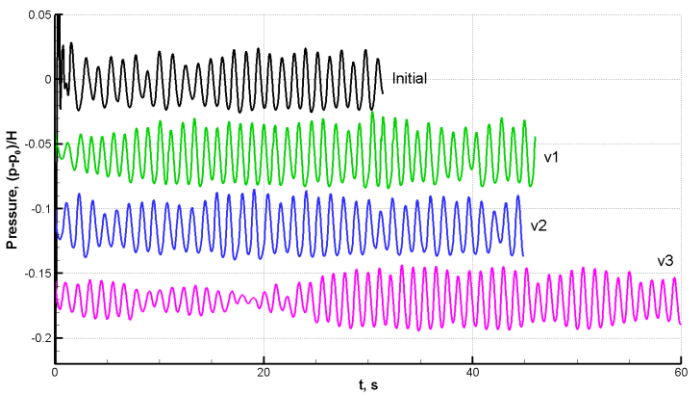

Figure 8. Pressure pulsations in WG inlet.

6. Runner shape variation

The shape of runner blades, hub, and shroud effectively control velocity profile downstream the runner, and therefore the flow pattern in the draft tube. Side effect of runner modifications is possible reduction in efficiency and possible shift of the efficiency hill-chart to lower or higher flow-rates. At the stage of runner design significant deviation from target values is not allowed. Therefore prior to investigation of the effect of runner geometry on the intensity of high load oscillations, the set of admissible runner modifications should be outlined or generated. Namely, all considered runner modifications should be comparable to the initial (or target) runner in terms of efficiency and cavitation. It means that the position of best efficiency point on turbine hill-chart and the level of efficiency should be preserved or at least not deteriorated. The same should be met for cavitation.

In order to construct the set of admissible runner shapes, fulfilling this principal requirement, we used our in-house runner optimization tool [12]. The runner with high self-exited pressure oscillations was taken as initial. Two operating point 3-objective optimization was carried out, aimed at increasing turbine efficiency in part load and high load, as well as minimization of cavitation at high load. Part load and high load operating points were set by their dimensionless guide vane openings A_0=0.414 and A_0=0.608, respectively.

Runner shape was parameterized with 23 free geometrical parameters, involving angular coordinate of the blade and meridian projection of the blade and hub [12]. Multi-objective genetic algorithm (MOGA) is used to find the solution of optimization problem. Several thousand runner modifications were constructed and computed to find the converged Pareto front. Flow analysis of each runner modification is performed in frames of steady state periodic stage approach in computational domain, including wicket gate, runner and draft tube.

Fig. 9 shows Pareto front, obtained after 20 generations of MOGA. The values of efficiency in part load (η_1) and full load (η_2) are normalized by BEP efficiency of turbine with the initial runner. This set was used as the source pool of runner modifications. Four runner modifications M1, M2, M3, M4, marked in Fig. 9, were selected from Pareto front for further analysis. All of them outperform the initial runner in terms of efficiency and cavitation. Fig. 10 illustrates significant variation of the runner blade. In order to prove high efficiency of the modified runners, Fig. 11 shows the computed efficiency hill-charts. It can be seen, that all runner modifications significantly outperforms the initial one, especially in high load operating point (by 1 ÷ 2%).

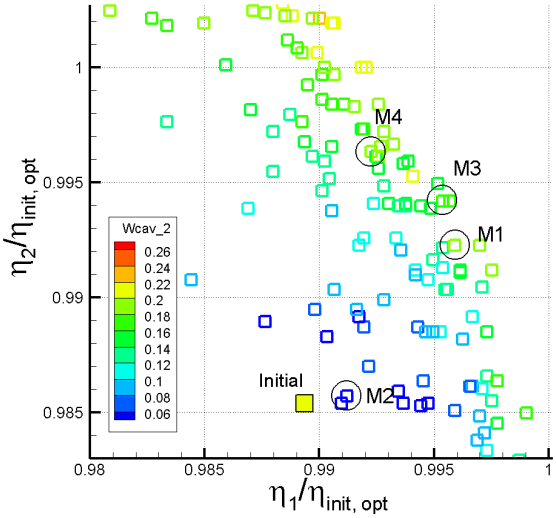

Figure 9. Projection of 3D Pareto front on the plane of efficiency objective functionals.

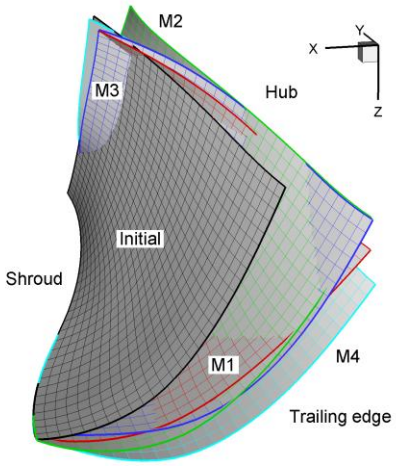

Figure 10. Comparison of runners in meridian projection.

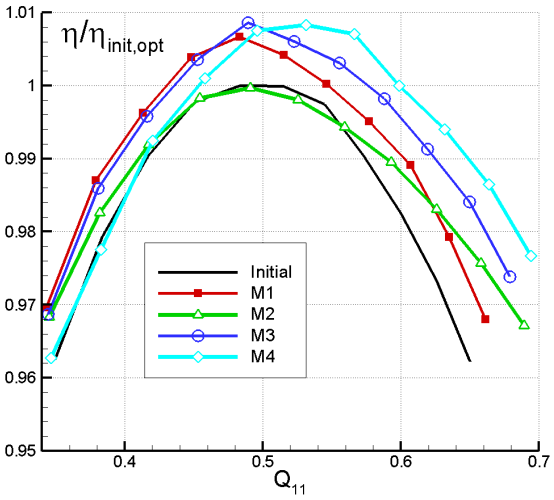

Figure 11. Computed efficiency hill-charts.

Then, unsteady CFD analysis of the selected modifications was performed, using the 1D-3D two-phase model, described in section 2. Air was not injected ($\alpha_G \equiv 0$). Fig. 12 shows the resulting pressure oscillations, computed for constant guide vane opening A_0=0.608. Pressure levels are shifted for the sake of visualization. The amplitude of pulsations as function of relative power is shown in Fig. 13. It can be seen, that all runner modifications have smaller amplitude of pressure pulsations, than the initial one. Among the modified runners, M2 and M4 have 3 times smaller pulsation amplitudes, than M1 and M3 do.

In order to explain different dynamic behaviour of the considered runners, the analysis of velocity profiles is carried out. Fig. 14 illustrate steady state velocity profiles downstream the runner, circumferentially averaged and extracted in section S1, shown in Fig. 7. Correlation is clearly seen between the amplitude of pulsations and the shape of axial and circumferential velocity profiles. Velocity profiles of M1 and M3 runners are close to each other, resembling the profiles of the initial runner. While M2 and M4 are different, with increased axial velocity and decreased negative swirl near the hub.

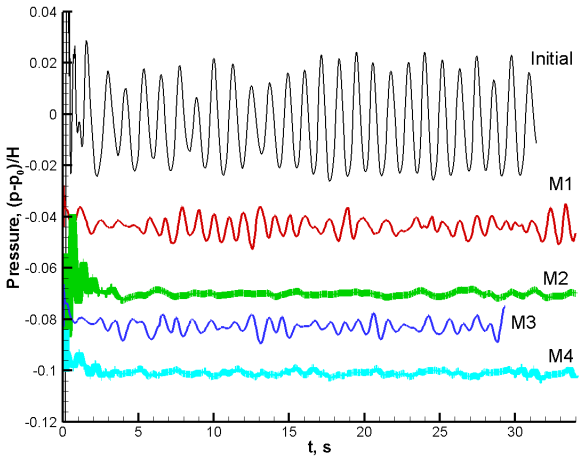

Figure 12. Pressure pulsations in WG inlet at $P/P_{rated} \sim 1.2$.

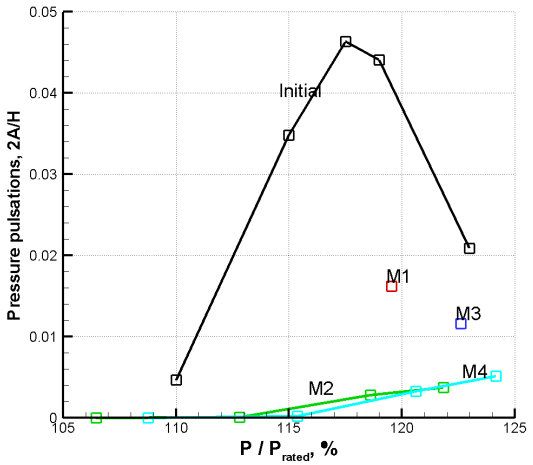

Figure 13. Amplitude of pressure pulsations as function of relative power.

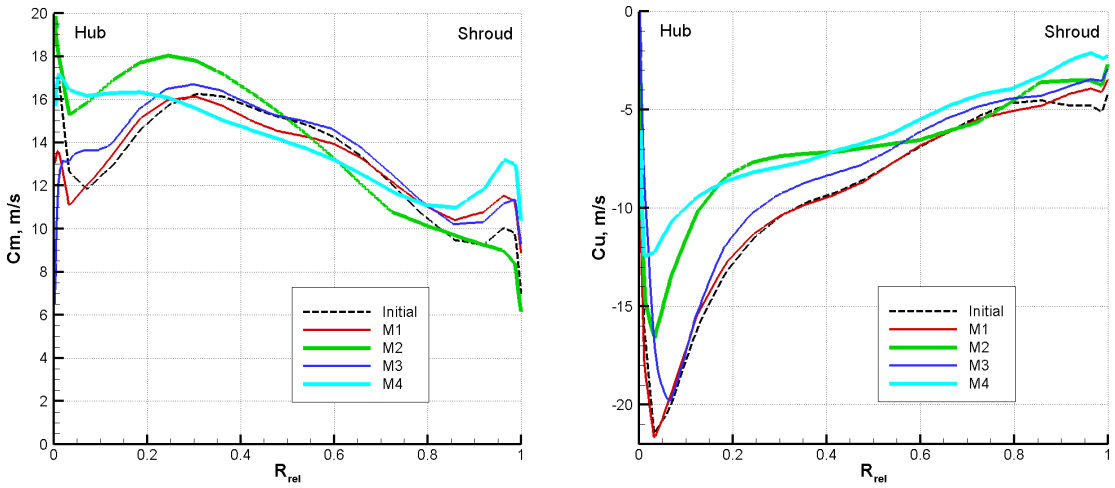

Figure 14. Meridian and circumferential velocity profiles downstream the runner at $P/P_{rated} \sim 1.2$.

7. Conclusion

Previously developed 1D-3D CFD model of full load pulsations is further advanced and applied to investigation of countermeasures, used in practice to suppress or eliminate high load instability and associated pressure oscillations. First, the third phase – non-condensable gas – is incorporated into the model in order to simulate air injection. Simple incompressible air model is used for the beginning. This model is applied to investigate the effect of air injection through the runner shaft. CFD computations confirm that air injection reduces the amplitude of pressure pulsations. The reason is the reduction of cavitation zone in the center of the draft tube. Sufficient air injection at constant flow-rate $Q_{air}/Q \sim 0.004$ reduces the amplitude of high load pulsations in several times. In future more accurate compressible air model should be used in order to account the change in cavity compliance.

Then, 2-phase "liquid-vapor" model is used to investigate the effect of runner cone shape. Computations show, that the shape of runner cone has negligible effect on pressure pulsations at high load.

Investigation of the effect of runner shape is the most interesting, since it allows flexible variation of draft tube inlet velocity profile. Several runner modifications were analyzed, comparable or superior to the initial runner in terms of efficiency and cavitation. The results show that high load instability can be eliminated without the need of air injection. Correlation is found between the velocity profiles downstream the runner and the intensity of full load oscillations. This has to be accounted on at runner design. More detailed investigations, both numerical and experimental, are needed.

Acknowledgments

This work was partly supported by grant №14-01-00278 of Russian Foundation for Basic Research.

Nomenclature

a	Wave speed in the penstock [m/s]	P	Power [MW]
A	Penstock cross section [m^2]	Q	Discharge [m^3/s]
A_0	Dimensionless guide vane opening [-]	V_c	cavity volume [m^3]
C	Cavity compliance [m^2]	α_L	Liquid volume fraction [-]
E	Total specific energy [m]	α_G	Air volume fraction [-]
g	Gravity acceleration [m/s^2]	ρ	Mixture density [kg/m^3]
H	Net head [m]	ρ_L	Water density [kg/m^3]
h	Piezometric head ($= p/\rho_L g - z$) [m]	ρ_V	Vapor density [kg/m^3]
p_V	Vapor pressure [Pa]	ρ_G	Air density [kg/m^3]

References

[1] Jacob T and Prenat J-E 1996 Francis Turbine Surge: Discussion and Data Base *IAHR Symp. on Hydraulic Machinery and Systems* (Valencia, Spain)
[2] Koutnik J, and Pulpitel L 1996 Modeling of the Francis turbine full-load surge *Modeling, Testing and Monitoring for Hydro Power plants* (Lausanne, Switzerland).
[3] Dörfler P 2009 Evaluating 1D models for vortex-induced pulsation in Francis turbines *Proceedings of 3rd IAHR Working Group on Cavitation and Dynamic Problems in Hydraulic Machinery and Systems* (Brno, Czech Republic) **2** pp 315-324
[4] Chirkov D, Avdyushenko A, Panov L, Bannikov D, Cherny S, Skorospelov V, Pylev I 2012 CFD simulation of pressure and discharge surge in Francis turbine at off-design conditions *IAHR Symp. on Hydraulic Machinery and Systems* (Beijing, China)
[5] Chirkov D, Panov L, Cherny S, Pylev I 2014 Numerical simulation of full load surge in Francis turbines based on three-dimensional cavitating flow model *IAHR Symp. on Hydraulic Machinery and Systems* (Montreal, Canada)
[6] Chirkov D, Cherny S, Scherbakov P, Zakharov A 2015 Evaluation of range of stable operation of hydraulic turbine based on 1D-3D model of full load pulsations *Proceedings of 6th IAHR Working Group on Cavitation and dynamic problems in hydraulic machinery and systems* (Ljubljana, Slovenia) pp 177–184
[7] Papillon B, Kirejczyk J, Sabourin M 2000 Atmospheric air admission in hydro turbines *Hydrovision* paper 3C
[8] Dörfler P, Sick M, Coutu A 2013 *Flow-Induced Pulsation and Vibration in Hydroelectric Machinery* (London: Springer-Verlag) 242 p
[9] Türkmenoglu V 2013 The vortex effect of Francis turbine in electric power generation Turk J Elec Eng & Comp Sci 21 pp 26-37
[10] Kunz R F, Boger D A, Stinebring D A et al 2000 A preconditioned Navier-Stokes method for two-phase flows with application to cavitation prediction *Computers & Fluids* **29** pp 849–75
[11] Dörfler P K, Braun O, Sick M 2011 Hydraulic stability in high-load operation: a new model and its use in Francis turbine refurbishment *Hydropower & Dams* **4**, pp 84-88
[12] Lyutov A E, Chirkov D V, Skorospelov V A, Turuk P A, Cherny S G 2015 Coupled Multipoint Shape Optimization of Runner and Draft Tube of Hydraulic Turbines *ASME Journal of Fluids Engineering* **137** No. 111302
[13] Coutier-Delgosha O, Fortes-Patella R, and Reboud J L 2003 Evaluation of the turbulence model influence on the numerical simulations of unsteady cavitation Journal of Fluids Engineering 125 No. 1 p. 38-45.
[14] Chen Y S, and Kim S W 1987 Computation of turbulent flows using an extended k-ε turbulence closure model. NASA CR-179204.
[15] Zwart P J, Gerber A G, Belamri T A 2004 Two-phase flow model for predicting cavitation dynamics. ICMF 2004 International Conference on Multiphase Flow. Paper No. 152 (Yokohama, Japan).
[16] Susan-Resiga R, Vu T C, Muntean S, Ciocan G D, Nennemann B 2006 Jet Control of the Draft Tube Vortex Rope in Francis Turbines at Partial Discharge *IAHR Symp. on Hydraulic Machinery and Systems* (Yokohama, Japan)
[17] Bosioc A I, Tanasa C, Muntean S and Susan-Resiga R F 2010 Unsteady pressure measurements and numerical investigation of the jet control method in a conical diffuser with swirling flow *IAHR Symp. on Hydraulic Machinery and Systems* (Timisoara, Romania)
[18] Panov L V, Chirkov D V, Cherny S G, Pylev I M and Sotnikov A A 2012 Numerical modeling of steady-state cavitational flow of viscous fluid in Francis hydroturbine *Thermophysics and Aeromechanics* **19**, No. 3 pp 415-427
[19] Feng J J, Li W F, Wu H, Lu J L, Liao W L, and Luo X Q, 2014 Investigation on pressure fluctuation in a Francis turbine with improvement measures *IAHR Symp. on Hydraulic Machinery and Systems* (Montreal, Canada)